Available online at www.sciencedirect.com
SCIENCE DIRECT®
Journal of Nuclear Materials 322 (2003) 36–44
journal of nuclear materials
www.elsevier.com/locate/jnucmat

High corrosion resistant Ti–5%Ta–1.8%Nb alloy for fuel reprocessing application

K. Kapoor [a,*], Vivekanand Kain [b], T. Gopalkrishna [a], T. Sanyal [a], P.K. De [b]

[a] *Advanced Materials Characterizations Laboratory, Nuclear Fuel Complex, ECIL Post, Hyderabad-500 062, India*
[b] *Materials Science Division, Bhabha Atomic Research Center, Mumbai-400 085, India*

Received 28 February 2003; accepted 2 June 2003

Abstract

The conventional low carbon austenitic stainless steels display good corrosion resistance behaviour in nitric acid media. However, they are sensitive to intergranular corrosion in boiling nitric acid media in the presence of oxidizing ions like hexavalent chromium, tetravalent iron and hexavalent plutonium. The Ti–5%Ta–1.8%Nb alloy was evaluated as a candidate material for such applications of nuclear fuel reprocessing. Extensive tests were carried out to establish the superior corrosion properties in comparison to the conventional stainless steel or nitric acid grade stainless steel. The fabricability of this new alloy to various shapes like rod, sheet, wire and its weldability, which is required for making vessels, was found to be good.
© 2003 Elsevier B.V. All rights reserved.

1. Introduction

In the reprocessing plants highly oxidizing boiling nitric acid medium makes the conventional low carbon austenitic stainless steel unacceptable. They are sensitive to intergranular corrosion in boiling nitric media in the presence of oxidizing ions like hexavalent chromium, tetravalent iron and hexavalent plutonium. The polarization potential can shift to transpassive state with strong intergranular attack. For example, the acid recovery evaporator vessel of the Tokai Reprocessing Plant in Japan, which was fabricated from austenitic stainless steel, failed due to severe corrosion [1]. For applications in a highly oxidizing medium requiring high corrosion resistance special grades like Nitric Acid Grade (NAG) 304L perform better. Studies have been carried out to explore Zr, Ti and Ti–5%Ta as alternate to austenitic stainless steels [2–4]. In such applications suitability of a new titanium based alloy with 5.0%Ta and 1.8%Nb is explored. Its superiority with respect to the corrosion aspect in boiling nitric acid medium is studied and compared with conventional low carbon and NAG 304L stainless steel. It was found that the Ti–5%Ta–1.8%Nb alloy is a good candidate material for applications such as making vessels for nuclear fuel reprocessing.

Titanium base alloys are preferable over stainless steel, as these are highly oxidizable and possess outstanding corrosion resistance in many media especially in boiling nitric acid up to 98% concentration. A titanium-oxide film forms spontaneously in air, water, oxidizing and reducing media with even traces of oxygen present in the media. The oxide film is adherent and protects the metal from the corrosive solution. The film has good chemical stability for a wide range of pH values such as 4–12 [5]. Further the corrosion rate is unaffected by the metallurgical state of the material and unaffected by the presence of hexavalent chromium. In comparison with stainless steel, titanium-based alloy Ti–5%Ta–1.8%Nb should therefore have better corrosion and mechanical properties. Hence it can be considered a suitable candidate material for this critical application. The development of the Ti–5%Ta–1.8%Nb alloy,

* Corresponding author. Tel.: +91-40 27184091/7120151; fax: +90-40 27121209/27121305/7121209.
E-mail address: kapoork@nfc.ernet.in (K. Kapoor).

0022-3115/$ - see front matter © 2003 Elsevier B.V. All rights reserved.
doi:10.1016/S0022-3115(03)00302-7

comparative performance with other suitable materials, and characterisation of its microstructural, mechanical, welding and corrosion properties have been attempted in this study.

2. Process route

The process for the preparation of Ti–5%Ta–1.8%Nb alloy ingot was initiated by taking titanium (Ti) sponge, tantalum (Ta) and niobium (Nb) sheets. For making 4.5 kg compacts of Ti–5%Ta–1.8%Nb, it requires 4149 g of Ti, 81 g (1.8%) of Nb and 225 g (5%) of Ta. The sheets of Ta and Nb were cut to the required size, so that these elements amount to uniform content throughout the length of the electrode. The contents were compacted and vacuum arc remelted in three steps. After each remelting chemical analysis was carried out for checking the composition of alloying elements namely Nb, Ta using X-ray fluorescence technique [6] and for estimation of impurities in the ingots such as nitrogen, hydrogen and oxygen by inert gas fusion, and iron by atomic absorption spectrometry. The ingots of size 192 mm dia × 200 mm length were hot extruded to 30 mm dia rods. These rods were cold swaged to a size of 25 mm dia rod, which was followed by annealing at 923 K for 1 h. The rods were machined and cold rolled to sheets of size 100 mm wide × 2.5 mm thick. The rods and sheets were subjected to ultrasonic NDT examination for checking the soundness of the material. Also the rods were bench drawn to make wires for filler material for tungsten inert gas (TIG) welding. Weld samples by TIG were made from the sheets and consumable wires from same material.

In case of the SS 304L and SS 304L (NAG) grade material it was tested in as-received and sensitized condition (953 K/1 h/air cool). The composition of this material is given in Table 1. The SS 304L NAG grade steel is made by electro-slag-refining process, which results in very low level of inclusions and trace impurities. In case of nitric acid application this low inclusion steel resists intergranular corrosion much more than the conventional SS 304L grade.

3. Experimental

Table 2 gives the composition of the material. The composition of alloying elements in this material has been tuned to get the optimum metallurgical, corrosion and mechanical properties. The niobium present in the alloy helps in reducing the oxygen pickup and tantalum helps to improve the corrosion resistance of the material.

The mechanical property and structure evaluation at rod and sheet stage have been done for establishing the overall property of the material and to arrive at a suitable processing route to final sheet and wire shape. The weld sample was subjected to various weldability tests to ensure the material to be suitable for welded structural application.

Extensive corrosion tests were carried out in boiling nitric acid for this material, SS 304L and SS 304L (NAG). The samples were subjected to 10-day corrosion test as per ASTM A262, Practice C. The corrosion rate was evaluated in terms of weight loss during the exposure.

In case of the rod material, anodic polarization tests were carried out in 1 N HNO_3 solution deaerated by bubbling argon gas before and during the test. The scan rate used was 0.33 mV/s and the test was carried out at room temperature. The Ti–5%Ta–1.8%Nb alloy sample

Table 1
Chemical composition of SS 304L and SS 304L (NAG) grade steel

Element	SS 304L (NAG)		SS 304L	
	Specification	Analysis	Specification	Analysis
C	0.02% max	0.019	0.035% max	0.025%
Ni	10–11%	10.3%	8–13% max	12.2%
Cr	18–20%	19.1%	18–20%	19.5%
Mn	1.8% max	1.34%	2.0% max	1.5%
Si	0.3% max	0.19%	0.75% max	0.50%
P	0.02% max	0.016%	0.04% max	0.03%
S	0.01% max	<0.002%	0.03% max	0.02%
N	0.07% max	0.053%	Not specified	
Al	0.05% max	<0.02%	Not specified	
Cu	0.01% max	<0.038%	Not specified	
Mo	0.10% max	<0.10%	Not specified	
Ti	0.05% max	<0.05%	Not specified	
B	0.001% max	<0.001%	Not specified	
Co	0.05% max	<0.03%	Not specified	
O	0.008% max	<0.005%	Not specified	

Table 2
Chemical composition of Ti–5%Ta–1.8%Nb material

Element	Desired specification	Analysis
N	300 ppm (max)	25 ppm
C	1000 ppm (max)	200 ppm
H	150 ppm (max)	6 ppm
Fe	300 ppm (max)	210 ppm
O	900 ppm (max)	382 ppm
Ta	4–6 wt%	4.52%
Nb	1.8–2.0 wt%	1.82%

was mounted in a cold setting resin so as to expose the cross-sectional face of the alloy bar to the solution. The metallographic polishing was done on this face and the anodic polarization test was carried out from the open circuit potential to a potential of 1400 mV vs saturated calomal electrode (SCE). The reference electrode used in the testing was saturated calomal electrode. The relation between SCE and standard hydrogen electrode (SHE) is as follows:

$$\text{mV (SCE)} = +242 \text{ mV (SHE)}$$

The welded sample of Ti–5%Ta–1.8%Nb alloy was mounted in a cold setting resin, metallographically polished and masked so as to expose (i) the heat-affected zone (HAZ) and (ii) the weld pool region of the sample to the solution. The anodic polarization tests were carried out from the open circuit potential to a potential of 1600 mV (SCE). In case of the welded sample anodic polarization tests were carried out in 1 N HNO_3 solution deaerated by bubbling argon gas before and during the test. The scan rate used was 0.33 mV/s. All the tests were carried out at room temperature.

For comparison the SS 304L and SS 304L (NAG) were tested for anodic polarization behaviour under similar conditions.

The susceptibility to end grain corrosion of the rod, welded sample, SS 304L and SS 304L (NAG) was evaluated in 9 N HNO_3 + 1 g/l Cr^{6+} boiling solution for 24 h. The test was carried out for four periods of 24 h each and the solution was refreshed in each period. The weight loss was measured in each period and reported. The depths of the end grain attack from the cross-sectional face of the test specimen were measured after the test and are reported.

The susceptibility to intergranular corrosion in nitric acid environment is tested as per the standard practice C of A262, ASTM. This test employs a boiling solution of 65% nitric acid. The susceptibility to end grain corrosion was tested in a boiling solution of 9 N HNO_3 + 1 g/l Cr^{6+} because only highly oxidizing solutions would show the susceptibility to end grain corrosion. In service with stainless steel components, the reprocessing fluids (mainly nitric acids of different concentrations) would accumulate Cr^{6+} ions and become highly oxidizing in nature and cause end grain corrosion over a prolonged service time. In short term tests with even 65% nitric acid the susceptibility to end grain corrosion cannot be detected. For this reason a different solution containing Cr^{6+} ions is used for this test. The polarization test was carried out in 1 N HNO_3 solution. In a polarization test the potential is applied on the specimen and the aggressiveness of the test can be increased with applied potential. The applied potential (or increasing the concentration and temperature of the solution) increases the aggressiveness. This is a simple test to assess the passivation behaviour of materials and can be applied in any solution of interest.

4. Results

4.1. Microstructure and mechanical properties of the alloy

The microstructural evaluation was carried out at billet, extruded rod, final rod (after swaging and annealing), cold rolled and annealed sheet and weld stage. The as cast structure of the billet after vacuum arc melting shows coarse martensitic structure with plate type morphology, Fig. 1(a). The beta quenched billet showed fine martensitic structure with needle shaped morphology, Fig. 1(b). At the extruded rod stage elongated grains of the second phase (β) at the grain boundary are observed, Fig. 2(a) and (b). After cold swaging and annealing, the microstructure consists of fine equiaxed grains of average size 15 μm, Fig. 3. The second phase (β) is broken; quantitative analysis of its

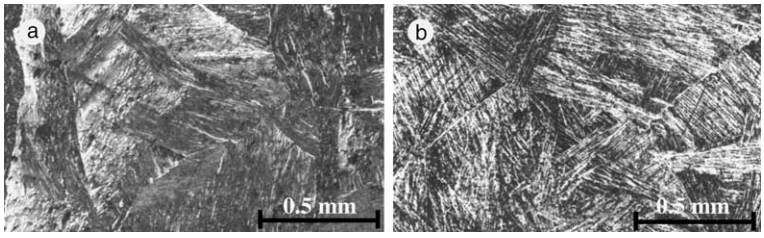

Fig. 1. Ti–5Ta–1.8Nb alloy optical microstructure: (a) as cast structure showing the acicular structure. (b) Heat treated at 1000 °C and water quenched (known as beta quench). Fine acicular structure observed (no second phase resolved).

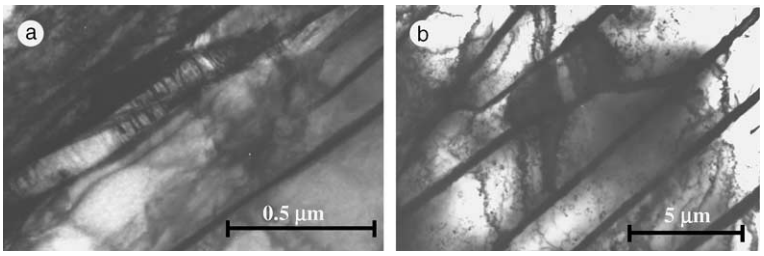

Fig. 2. Ti–5%Ta–1.8%Nb alloy transmission electron microscopy structure at extruded rod stage (longitudinal sections) at different magnifications. In TEM the fine alpha–beta lamellar structure is seen showing that extrusion is carried out in two-phase region.

size, density, morphology and volume fraction is given in Table 3. This β phase is rich in Ta and Nb; energy dispersive spectrum of the particle superimposed on the base material spectra is shown in Fig. 4. After cold rolling and annealing to sheet there is a modification of the grain size to 10 μm and β phase morphology and distribution (Fig. 5). The microstructure of sheet material is shown in Fig. 6, with size and volume fraction of β phase compared with that at the rod stage in Table 3. This sheet is welded using tungsten inert gas welding, the microstructure of the sheet and the weld region is shown in Fig. 7. The material shows fine structure of the base material with average grain size 10 μm, and coarse structure of fusion region. No β phase was observed in the fusion region.

Table 4 gives the mechanical properties of the rod material. The ratio of ultimate tensile strength to yield strength is very low 1.1 (cold worked), showing that the material has low strain hardening. The welded samples were subjected to bend (forward and reverse) test. No failure was observed with bend radius of 2 times thickness. Tensile specimens were made from weld and base material; these tensile properties are summarized in Table 4. From the results of the mechanical test carried out (Table 4) it is shown that the material has good weldability.

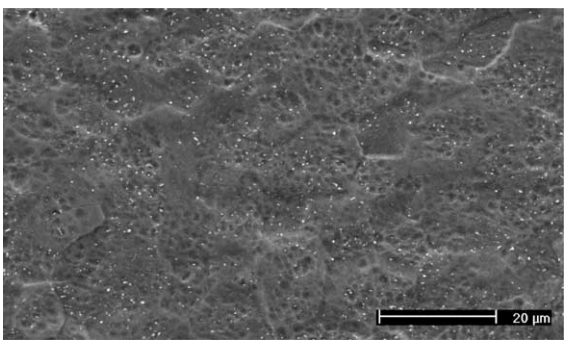

Fig. 3. SEM Micrograph of rod material (transverse section) with β phase precipitates.

4.2. Corrosion properties of the alloy

4.2.1. Boiling nitric acid test

Boiling nitric acid i.e. practice C, A262, ASTM tests were carried out on the rod material (as received and heat treated), base, heat-affected region and fusion region for the Ti-base alloy and the SS-grades. The results of practice C, A262, ASTM for this material are given in Table 5. These results were used along with the results of the anodic polarization tests to assess the resistance of this alloy in nitric acid environments. Also included are the test results of 304L, 304L (NAG) and reported results for Ti–5%Ta material. The corrosion rates observed were better than those for stainless steel grades and those reported for Ti–5%Ta material tested under similar conditions.

4.2.2. Anodic polarization in 1 N HNO_3 for the rod material

The anodic polarization curve of this alloy is shown in Fig. 8 and compared with the behaviour of type 304L (commercial purity) and type 304L NAG stainless steel in similar tests.

It can be seen from Fig. 8 that type 304L NAG shows the best passivity in this solution followed by the Ti–5%Ta–1.8%Nb alloy. The Ti–5%Ta–1.8%Nb alloy showed better passivity than type 304L (commercial purity) stainless steel in this test. It is also clear from Fig. 8 that the Ti–5%Ta–1.8%Nb alloy showed passivity even

Table 3
Morphology of β phase

S. no.	Material	Shape factor	Area (μm^2)	Volume (%)	Density (number/100 μm^2)
1	Rod	1.3	0.07	1.1	18
2	Sheet	1.0	0.16	0.9	6

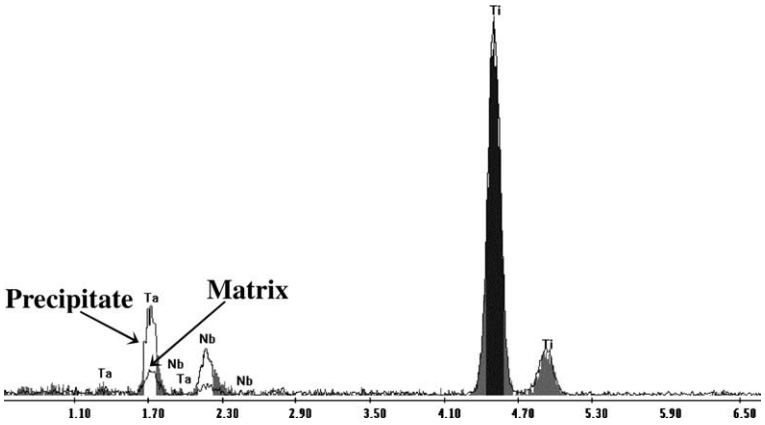

Fig. 4. Comparison of EDAX spectrum of precipitate and base material.

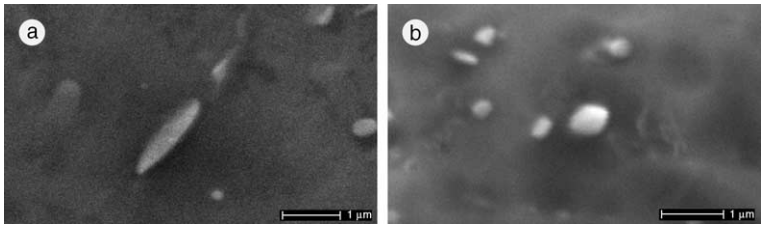

Fig. 5. SEM micrograph of β phase precipitates in (a) rod and (b) sheet material.

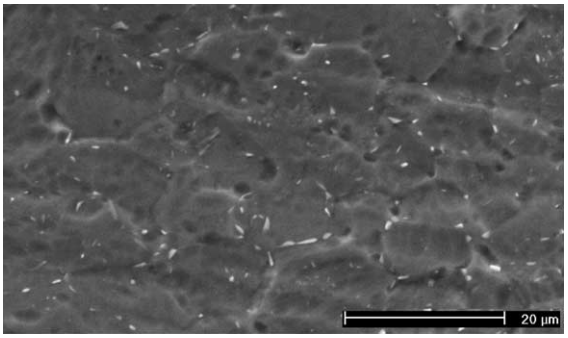

Fig. 6. SEM micrograph of sheet material (transverse section) with β phase precipitates.

up to a potential of 1400 mV (SCE) though the type 304L commercial purity and type 304L NAG stainless steels showed transpassivity soon after a potential of around 900–1000 mV (SCE). Therefore, the Ti–5%Ta–1.8%Nb alloy showed the best resistance in the test in the highly oxidizing (transpassive) conditions.

The specimen had developed a bluish film after the experiment. This could be due to the oxidizing nature of the material in the environment, forming the protective film.

4.2.3. Anodic polarization in 1 N HNO_3 for welded sheet material

The anodic polarization curve of the HAZ and the weld pool region of this alloy are shown in Fig. 9 and are compared with the behaviour of the as fabricated rod.

It can be seen from Fig. 9 that the cross-sectional surface of the alloy bar showed better passivity than the welded sample. In the welded sample, the HAZ and the weld pool showed similar behaviour. There was a deviation from passivity at around 1500 mV (SCE) though the current density values did not increase much even at a high potential of 1600 mV (SCE). Compared to type 304 stainless steels, this alloy did show stable passivity at high potentials. The current density of the welded sample did show increase in the passive range as compared to that for the fabricated bar.

4.2.4. The end grain corrosion test for rod material

The susceptibility to end grain corrosion is evaluated in highly oxidizing environments. Since the anodic polarization tests indicated that this material is resistant to corrosion in highly oxidizing environments, the end grain corrosion test was carried out. A highly oxidizing, concentrated nitric acid environment, containing hexavalent ions of chromium is expected to develop in contact with materials of construction after a prolonged

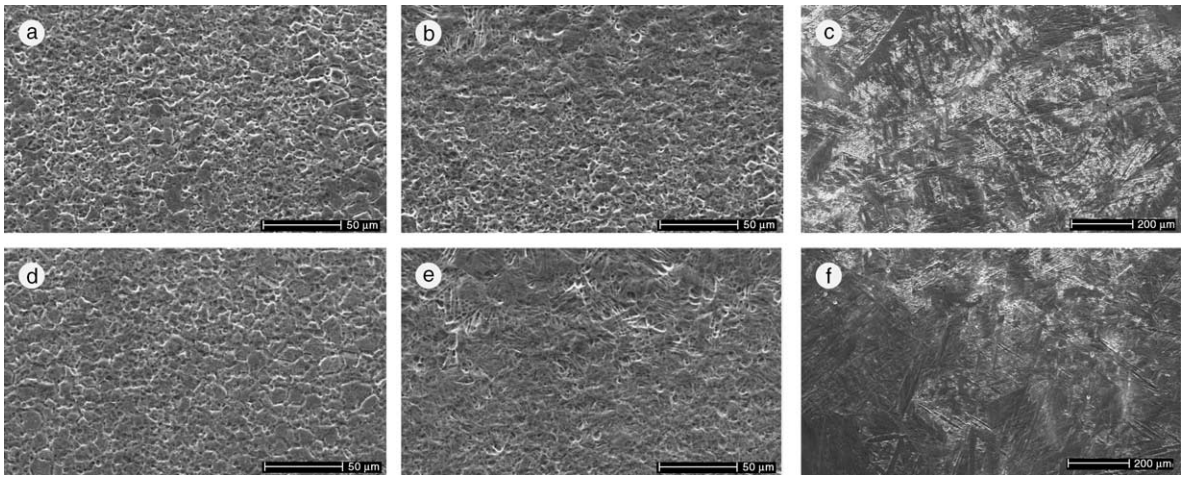

Fig. 7. SEM micrographs of Ti–5%Ta–1.8%Nb welded sheet material showing longitudinal section (a) base material, (b) heat-affected zone, (c) fusion zone, and transverse section (d) base material, (e) heat-affected zone, (f) fusion zone.

Table 4
Mechanical properties of Ti–5%Ta–1.8%Nb alloy

S. no.	Sample	UTS (MPa)	YS (MPa)	%EL (in 25 mm gage length)
1	Rod material	670	610	20.4
2	Base material	731	643	22.0
3	Weld region	463	400	31.0

Table 5
Results of the boiling HNO_3 test

S. no.	Sample		Corrosion rate (mpy)
1	Rod	Ti–Ta–Nb	1.24
2		Ti–Ta–Nb (sensitized 973 K/1 h)	1.24
3	Weld	Ti–Ta–Nb sheet base material	0.62
4		Ti–Ta–Nb HAZ	0.93
5		Ti–Ta–Nb fusion zone	0.78
6	Ti–5%Ta [9]		1.2
7	304L		9.6
8	304L (NAG)		4.8

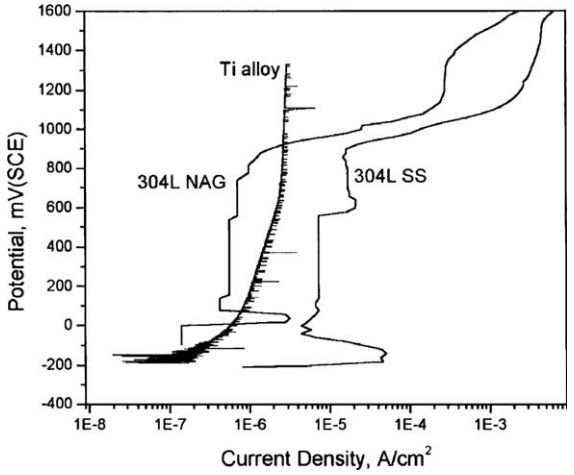

Fig. 8. Anodic polarization curve of the cross-sectional face of the Ti–5%Ta–1.8%Nb alloy in 1 N HNO_3 solution (deaerated) at room temperature. The anodic polarization curves of type 304L (commercial purity) and type 304L NAG stainless steels in the same conditions are also shown for comparison.

time in the nuclear reprocessing plants, especially in components like dissolvers. The end grain test on the rod material giving weight loss measured in each period is given in Table 6. The depth of the end grain attack measured from the cross-sectional face of the test specimen is reported in Table 6.

4.2.5. The end grain corrosion test for welded sheet material

The weight loss was measured in each period and the results are shown in Table 6. The sample containing the weld pool and HAZ on both sides was exposed to this test. The depth of the end grain attack from the cross-sectional face of the test specimen was measured after the test and are reported in Table 6. It can be seen that even the welded sample of the alloy showed high resistance to end grain corrosion in the oxidizing solution.

It is evident from these test results that the welded Ti–5%Ta–1.8%Nb alloy showed similar resistance to end grain corrosion in highly oxidizing environment of the test. The anodic polarization behaviour in 1 N HNO_3 solution showed that the welded sample does

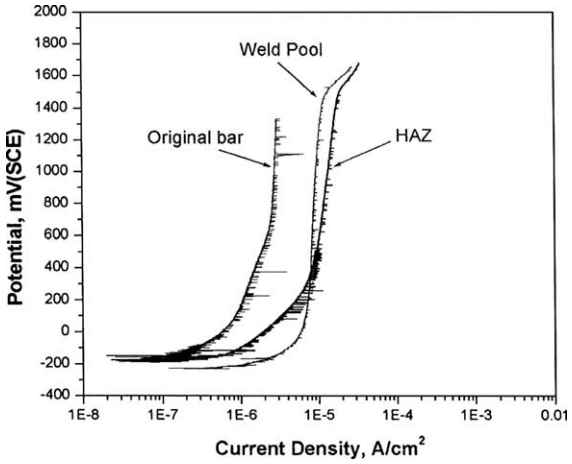

Fig. 9. Anodic polarization curve of the heat-affected zone (HAZ) and the weld pool region of the Ti–5%Ta–1.8%Nb alloy in 1 N HNO_3 solution (deaerated) at room temperature. The anodic polarization curves of the same alloy on the cross-sectional surface of the as fabricated bar in the same conditions is also shown for comparison.

have higher passivation current density. This indicates higher susceptibility to corrosion in the given medium.

In summary, the data on the anodic polarization (Figs. 8 and 9) and end grain corrosion tests (Table 6) carried out on Ti–5%Ta–1.8%Nb and its comparison with the type 304L (commercial purity), type NAG 304L stainless steels tested in similar test conditions has been generated and compared. The results show that the Ti–5%Ta–1.8%Nb alloy, in relation to the stainless steel grades, showed better passivity in nitric acid environments and high resistance to end grain attack in highly oxidizing solutions. Table 4 gives the results of ASTM A262, practice C, tests carried out on the three grades and reported value for Ti–5%Ta. The results of practice C, A262, ASTM are in line with the anodic polarization results and substantiate the superior corrosion resistance of Ti–5%Ta–1.8%Nb material.

The microstructure of the material was analysed after boiling nitric acid test. For this the metallographic samples from the heat-affected zone, fusion zone and base material were prepared. The specimens were boiled in the nitric acid in a glass basket to avoid any scratches

Table 6
Results of the end grain corrosion tests in 9 N HNO_3 + 1 g/l Cr^{6+} boiling solution for four periods of 24 h each for rod material, weld and 304L alloys

S. no.	Material	Corrosion rate (mpy)				Depth of end grain attack
		I	II	III	IV	
1	Ti–5Ta–1.8Nb alloy	0.80	0.60	0.17	0.17	No visible attack
2	Type 304L commercial purity	360	560	850	1020	500 μm
3	Type 304L nitric acid grade	570	620	705	770	250 μm
4	Welded Ti–5Ta–1.8Nb alloy	0.95	0.75	0.36	0.28	No visible attack

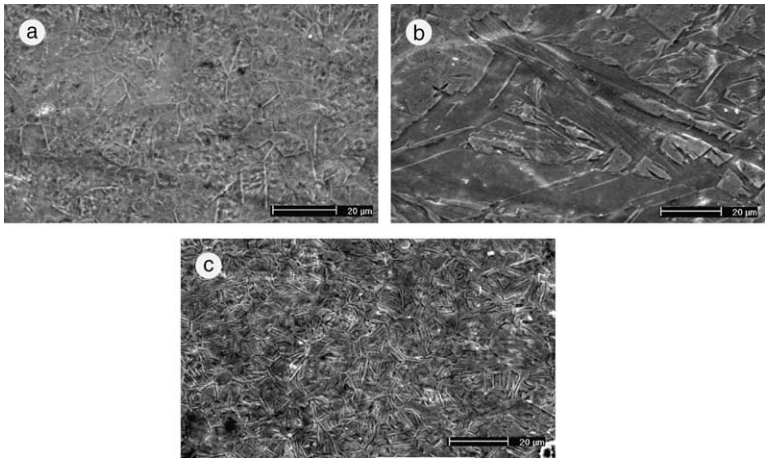

Fig. 10. SEM Micrograph of materials after 48 h boiling nitric acid test for (a) base material, (b) fusion zone and (c) HAZ showing no degradation of structure after the test.

during boiling. The test was carried out for 48 h and the microstructure was analysed in the three regions. Fig. 10 shows the microstructure in the three regions of the as-tested material, which shows no microstructure degradation in any of the three regions. In the base material surrounding the beta phase no signs of film breakage or localised attack was observed.

5. Discussion

It is reported that Ti–5%Ta is a single-phase alloy at room temperature [7]. Presence of second phase (β) has not been reported in this alloy. This composition is just within the α phase boundary at room temperature [8]. Ta and Nb are both β stabilizers, with Nb being stronger than Ta. With addition of 1.8% Nb some quantity (nearly 1%) of β is retained as precipitates. With thermo-mechanical processing to sheet, this size of this phase (see Fig. 5) coarsens and it becomes spherical with average shape factor of 1.0 as against 1.32 in the cold swaged and annealed condition. Its average number density decreases from 18 nos/100 μm^2 to 6 nos/100 μm^2. The fusion zone in the weld region has no such precipitates.

In the anodic polarization test, the weld pool and the heat-affected region showed higher current density than that for the base sheet material (Fig. 9). This is also reflected in the results of the boiling nitric acid (Huey) test as given in Table 4. This may be attributed to the difference in microstructure at the weld pool and presence of residual stresses at the heat-affected regions. The weld pool has an acicular structure (Fig. 7) that is coarse in the center of the weld pool and fine acicular towards the weld pool–base metal interface. The heat-affected region has coarser grains compared to the base sheet material (Fig. 7). The beta phase could not be resolved in both the weld pool and the heat-affected regions. This could be due to exposure of these regions to high temperatures during welding. The base sheet material does contain about 0.9 vol.% beta phase (Table 3). Another factor causing slightly higher corrosion rates at the heat-affected regions could be the presence of residual stresses. Welding invariably leaves residual stresses in the heat-affected regions due to thermal/solidification stresses. This does not change the structure of the material here but can cause a difference in the corrosion behaviour as it affects development of surface oxide film on these regions. It can be inferred from the results presented above that the beta phase is not harmful in strongly oxidizing mediums and, as in this case in boiling HNO_3 medium, may be helpful in developing better passivity. This is a new observation and may be explained as follows:

Titanium itself shows high corrosion resistance in nitric acids. Unalloyed titanium has been used extensively for handling and producing nitric acid in applications in which stainless steels have experienced significant uniform or intergranular corrosion [10]. Titanium offers an excellent resistance over the full concentration range at sub-boiling temperatures. As temperatures exceed 353 K, however, the corrosion resistance becomes highly dependent on nitric acid purity.

Limited corrosion testing of alpha–beta and beta titanium alloys in boiling nitric acid indicates that increasing aluminum and beta alloying elements tend to decrease corrosion resistance. Alpha alloys are generally most resistant to hot nitric acid.

Both Ta and Nb are strong beta stabilizers. However, both Ta and Nb show strong resistance to nitric acid (better than that of titanium alone).

Niobium is completely resistant to nitric acid in all concentrations at temperatures below 373 K. Even in 70% nitric acid at 523 K, it has a corrosion rate of only 0.025 mm/yr (1 mpy) [11]. In chromium plating solutions, niobium exhibits only a slight-weight change, and in the presence of small amounts of fluoride (F^-) catalyst, its corrosion resistance exceeds that of tantalum.

Tantalum is inert to nitric acid solutions in all concentrations and at all temperatures up to boiling. The presence of Cl^- in nitric acid does not reduce the corrosion resistance of the metal to this acid. The corrosion rate of tantalum to nitric acid at sub-boiling temperatures is less than 0.4 μm/yr (0.015 mpy) for most concentrations and temperatures. In general, the use of tantalum at these temperatures would not be economical, considering the resistance offered by stainless steels. At temperatures near and above the normal boiling point of nitric acid, the superior resistance of tantalum becomes pronounced.

Considerable data have been accumulated on the corrosion resistance of tantalum–titanium alloys. Dilution of tantalum with titanium shows considerable promise for the possibility of providing a lower cost alloy with corrosion resistance almost comparable to that of tantalum in some select environments. In addition to dilution with a lower cost material, the resulting marked reduction in density is particularly advantageous, because corrosion applications generally require materials on a volume rather than a weight basis. Corrosion tests in 10–70% nitric acid at the boiling point and at 463 K in sealed glass tubes were conducted on tantalum–titanium alloys ranging from pure tantalum to Ta–90Ti. All of these materials exhibited excellent behaviour, with corrosion rates less than 0.025 mm/yr (1 mpy) [11] and no indication of embrittlement.

Therefore, the beta phase that is present in the material under investigation and shown to contain enrichment in Nb and Ta shows better corrosion resistance. The beta phase of pure titanium is reported to show lesser corrosion resistance than that of the alpha phase. However, in the alloy under investigation the chemical

composition of the beta phase is different (Fig. 4) and the Ta and Nb present in the beta phase are what gives good corrosion resistance to it.

6. Conclusions

1. It is evident from these test results that the Ti–5%Ta–1.8%Nb alloy showed the best resistance to corrosion at transpassive potentials and to end grain corrosion in highly oxidizing environment of the test. This alloy is therefore expected to show very good resistance to corrosion in highly concentrated and oxidizing nitric acid environments containing corrosion products developed after a prolonged period of operation of the reprocessing plants. Further it has a potential to replace the conventional stainless steel 304L and 304L (NAG) for such application.
2. The Ti–5%Ta–1.8%Nb has good fabrication properties and can conveniently be converted into sheets, rods and wires meeting the desired properties. It has also good weldability required for making vessels for reprocessing plants.
3. The results show that the welded sample of Ti–5%Ta–1.8%Nb alloy showed passivity in nitric acid environments and high resistance to end grain attack in highly oxidizing solutions. A comparison of the anodic polarization behaviour of the heat-affected zone and weld pool region of the welded sample shows higher passivation current density than the original bar, though the absolute values of the current density remained very low.
4. The conventional Ti–5%Ta alloy is a single-phase alloy. With addition of Nb the beta phase is stabilized in the alloy, which is helpful in developing better passivity as observed in the anodic polarization tests. The chemical composition of the beta phase shows enrichment of Ta and Nb, which gives good corrosion resistance to this alloy in two-phase.

Acknowledgements

Authors acknowledge keen interest and guidance by Dr C. Ganguly, Chief Executive, Nuclear Fuel Complex, Hyderabad, India and kind permission to publish this work. Help by Dr Padmaprabu for assistance during microstructure evaluation is acknowledged. Authors gratefully acknowledge the useful discussions with the colleagues from IGCAR, Kalpakkam, India.

References

[1] N. Tsuji, K. Ishikawa, Y. Kishimoto, S. Hayashi, in: International Conference on Nuclear Fuel Reprocessing and Waste Management, Paris (France), 23–27 August, 1987; Nuclear Fuel Reprocessing and Waste Management, Society of French Nuclear Energy, 75 Paris (France), Vol. 3, 1987, 391, p. 1203.
[2] T. Furuga, H. Satoh, K. Shimogori, Y. Nakamura, K. Matsumoto, Y. Komori, S. Takeda, in: ANS International Topical Meeting on Fuel Reprocessing and Waste Management, Jackson Hole, WY (USA), 26–29 August 1984; Fuel Reprocessing and Waste Management, LaGrange Park, IL (USA), American Nuclear Society, Vol. 1, 1984, p. 249.
[3] U.K. Mudali, R.K. Dayal, J.B. Gnanamoorthy, J. Mater. Eng. Perform. 4 (6) (1995) 756.
[4] T. Seiichiro, N. Takayuki, K. Tsutomu, H. Shotaro, in: International Conference on Nuclear Fuel Reprocessing and Waste Management, Sendai (Japan), 14–18 April 1991; Proceedings of the Third International Conference on Nuclear Fuel Reprocessing and Waste Management, Japan Atomic Industrial Forum, 1991, 1186, p. 555.
[5] A. Takamura, K. Arakawam, Y. Moriguchi, in: R.I. Jaffee, N.E. Promisel (Eds.), The Science, Technology and Application of Titanium, Proceedings of the International Conference, Pergamon, Oxford, 1968, p. 209.
[6] G. Radha Krishna, H.R. Ravindra, B. Gopalan, S. Syamsundar, Anal. Chim. Acta 299 (1994) 285.
[7] T. Yamamoto, S. Tsukui, S. Okamota, T. Nagai, M. Takeuchi, S. Takeda, Y. Tanaka, J. Nucl. Mater. 228 (1996) 162.
[8] K. Thaddeus (Ed.), Binary Alloy Phase Diagrams, ASM Publication, Materials Park, OH, USA, 1986, p. 2100, and 1702.
[9] L. David, L. Lawrance (Eds.), Corrosion, 9th Ed., ASM Handbook, Vol. 13, ASM Publication, Materials Park, OH, USA, 1998, p. 679.
[10] L.C. Gilbert, C.W. Fink, Mater. Prog. (1956) 93.
[11] B.D. Craig, D.S. Anderson (Eds.), ASM Handbook of CORROSION DATA, 2nd Ed., ASM Publication, Materials Park, OH, USA, 1995, p. 543.